5-2014

Evaluation of Novel Multi-Dimensional Tissue Culturing Methods Using Autonomously Bioluminescent Human Cell Lines

James Dean Webb
jwebb39@utk.edu

Evaluation of Novel Multi-Dimensional Tissue Culturing Methods Using Autonomously Bioluminescent Human Cell Lines

James Dean Webb

Department of Ecology and Evolutionary Biology
The Center for Environmental Biotechnology
The University of Tennessee-Knoxville

Abstract

Bioluminescent imaging (BLI) systems possess several benefits over their fluorescent counterparts, including negligible interference from target tissues, and are therefore prevalently used in cellular and molecular research. Furthermore, a recently created human cell line expressing the bacterial luciferase (*lux*) gene cassette has resulted in autonomous bioluminescent production without the addition of exogenous substratrate or cell lysis. This BLI's ability to monitor cellular events on an extended basis and a notable deep tissue detectability may prove particularly applicable for evaluating previously difficult to image systems such as 3D tissue culturing techniques. These platforms attempt to mimic natural *in vivo* conditions, facilitating cell-to-cell contact and extracellular matrix (ECM) dynamics. In this research, several 3D culture techniques signifying a diverse coverage of available varieties were evaluated, ranging from magnetic levitation to gel encapsulation. Detectable bioluminescent signals were observed for all of the 3D culture techniques. These results demonstrate the feasibility of the *lux* BLI for this application, permitting the evaluation of 3D cellular dynamics for both short term and long term investigations.

Introduction

The development of bioluminescent imaging (BLI) systems throughout the previous decades has transformed the biotechnical and biomedical sciences. These systems harness bioluminescence, the production of light from a living organism through biochemical reactions, to visualize a diverse range of biological and chemical processes within a living system. This process, which is accomplished through the use of an oxidative, light producing enzyme such as firefly, *Renilla*, or bacterial luciferase, has become increasingly popular as a diagnostic tool within the scientific community compared to its fluorescent counterpart due to the complete absence of endogenous bioluminescence in tissue[1]. In contrast, background fluorescence from the myriad of autoflourescent molecules found within biological structures is commonly encountered as interference, severely limiting the fluorescent imaging's capabilities[2]. The near background-free nature of BLI therefore provides a characteristically more sensitive means of detection[3].

These highly sensitive, high resolution BLI systems are therefore particularly well suited to use in *in vivo* studies. Utilizing the bacterial bioluminescence *lux* cassette, researchers are capable of monitoring cellular events on a repeated and extended basis whereas traditional, enzymatic techniques are limited to providing only single data points at selected time points or upon completion of the event[4]. For example, TUNEL and MTT assays, commonly used to assess cell viability, necessitate the destruction of the sample by formaldehyde fixation and potential mutagenesis, respectively.

In particular, bacterial bioluminescence (*lux*) has recently been demonstrated as a powerful imaging tool via the creation of an autonomously bioluminescent human cell line[5]. Unlike firefly or *Renilla* luciferase-based systems, this cell line does not require the addition of an exogenous

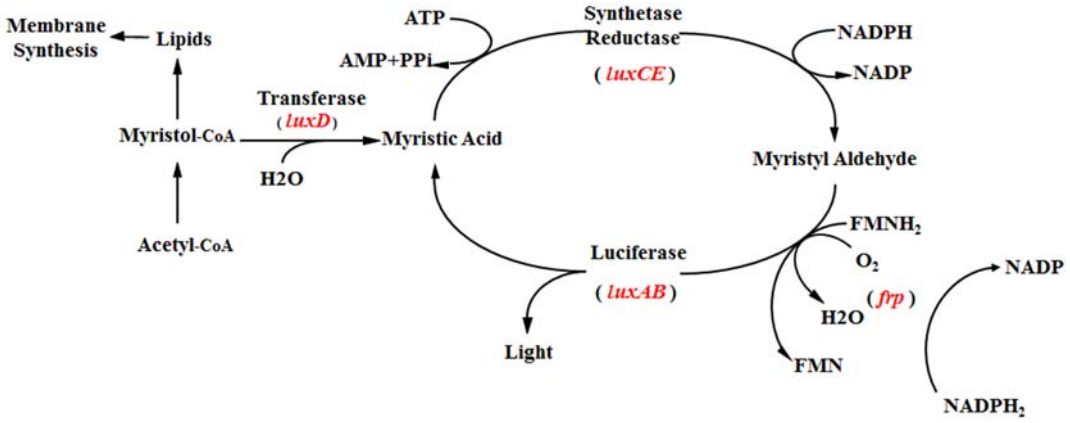

Figure 1. Schematic demonstrating the biochemical pathways and intermediates through which the *lux* cassette produces a bioluminescent signal that peaks at 490 nm.

substrate to initiate production of a detectable signal. Instead, the *lux* gene cassette synthesizes both the light production luciferase enzyme, as well as the entire assemblage required for substrate production and regeneration. In combination with abundant metabolites and membrane precursors, this architecture therefore permits the fully autonomous generation of a bioluminescent signal (Figure 1).

Other demonstrated benefits of this system include non-invasive *in vivo* compatibility and a defined quantitative correlation between signal strength and cell number. These traits are

relatively unique to the *lux* system, as several studies focusing on the alternative BLI luciferases have demonstrate that they are comparatively volatile in mammalian systems due to thermoinstability (measured half-lives of several minutes) and rapidly consuming their required substrate, compelling prompt evaluation[6, 7]. On the other hand, the stable and consistent activity of the *lux* cassette permits a particularly accurate correlation between the number of cells and the bioluminescent signal strength[8]. Using this relationship, researchers can therefore more precisely investigate the dynamics of cell growth in a non-destructive and continuous manner. Furthermore, recent optimization of this system has resulted in a dramatic increase in bioluminescent signal intensity as compared to the originally published *lux* system, permitting signal detection at lower cell concentrations and in deep tissue experiments[9].

Nevertheless, it is important to note that several disadvantages remain with respect to bacterial bioluminescence as compared to other BLIs. The most pertinent of these is that the resultant signal intensity of the *lux* reaction is significantly less than that produced by firefly luciferases, even when optimized *lux*-expressing cell lines are employed[10]. Similarly, the 490 nm wavelength of the *lux* signal maintains a greater propensity for absorption in animal tissues, requiring bacterial bioluminescence-based experiments to employ exceptionally sensitive imaging equipment and further increasing the difficulty of signal detection compared to other substrate-requiring luciferase systems[8].

An important application of the *lux* BLI is a more in-depth evaluation of systems that traditional technology were unable to assess. For example, one of the principal goals of contemporary tissue culture research has been to develop platforms that mimic natural *in vivo* conditions for use as experimental analogs. Since standard monolayer tissue culturing methods lack several of the characteristic features of natural tissue such as omnidirectional cell-to-cell contact, extracellular matrix (ECM) interactions, and the structural influences on gas/nutrient diffusion and transport, multi-dimensional or 3D culturing methods have garnered attention as potential alternatives[11, 12]. Nevertheless, these novel systems remain mostly unevaluated because of imaging difficulties and thus, have not become widely employed[13]. The depth and complex nature of these platforms have limited the feasibility of most imaging techniques because comprehensive and accurate analysis of 3D biological structures would require a strong signal-to-noise ratio (minimal interference from target) and significant tissue penetration[14].

In response to these challenges, this research endeavors to evaluate several of the novel culturing techniques using the previously developed autonomously bioluminescent human cell line. Demonstrating the capabilities of this BLI for 3D tissue culture imaging, its characteristic low background and deep tissue detectability should be compatible with evaluating previously difficult to image samples. Furthermore, the culturing techniques assessed represent a diverse range of 3D structure and a sound depiction of potential applications.

Materials and Methods

Cell growth and maintenance

Cell lines used in this study included a 1st generation *lux*-expressing autobioluminescent HEK293, a 2nd generation autobioluminescent HEK293 cell line that displayed a higher signal intensity compared to its 1st generation counterpart, and an autobioluminescent human colorectal carcinoma HCT116 cell line. HEK293 and HCT116 cells were grown, respectively, in Dulbecco's Modified Eagle Medium (DMEM) and McCoy's 5A medium (Hyclone), supplemented with 10% fetal bovine serum (FBS) (Hyclone), 1x sodium pyruvate (Life Technologies), 1x antibiotic/antimycotic (Life Technologies), 1x non-essential amino acids (Life Technologies), and Neomycin G418 (EMD Millipore) at a final concentration of 500 µg/ml G418 (750 µg/ml for HCT116). Cells were incubated at 37 °C with 5% CO_2. Medium was refreshed approximately every three to four days. Cells were passaged upon reaching 80% confluence.

Porous Polycaprolactone Scaffold (Kiyatec)

Actively growing 1st generation autobioluminescent HEK293 cells were harvested from a 75 cm^2 tissue culture flask. Cell number was then determined using a hemocytometer with a Trypan Blue vital stain. Approximately 3.0×10^5 cells were plated in triplicate onto a non-tissue culture treated 24-well plate, a non-tissue culture treated 24-well plate housing the polycarprolactone 3D scaffold (Kiyatec), and a tissue-culture treated 24-well plate to mimic suspension, 3D tissue scaffold, and monolayer culturing conditions, respectively. After a 2 hour incubation at 37 °C with 5% CO_2 to allow for cellular attachment to the scaffold and tissue culture-treated surface, medium in the scaffold and monolayer culture was refreshed to remove any unattached cells. Bioluminescence was then monitored using an IVIS Lumina imaging system (Perkin Elmer) using a 10 minute integration at 15 minute intervals for 24 hours.

Hyaluronic Acid Gel (Celenys)

Following Celenys's provided protocol, 24 hyaluronic hydrogels were plated in individual wells of a Ultra-Low binding 96-well plate (Corning) with 100µl of serum-free medium and incubated at 37 °C in a 5% CO_2 environment for 72 hours to permit liquid absorption and gel expansion. Immediately prior to cell seeding, actively growing 2nd generation autobioluminescent HEK293 cells were harvested from a 25 cm^2 tissue culture flask and counted using the Scepter automated cell counter (EMD Millipore). Cells were then washed with PBS and resuspended in growth medium to a final concentration of 5×10^5 cells/ml. To seed cells to the hydrogels, the old medium was removed from 21 of the 24 hydrogels and replaced with 100 µl freshly prepared cell suspension containing approximately 1.0×10^5 cells. The remaining 3 gels were refreshed with fresh medium to serve as negative controls. The plate was then incubated for 24 hours at 37 °C with 5% CO_2 to permit cell attachment. After the 24 hour incubation, the medium was removed to eliminate unattached cells and 100 µl of fresh medium was added to each well. The plate was then incubated for 5 days at 37 °C with 5% CO_2 without refreshing medium, in order to avoid any potential disruption of 3D structure formation. Following the 5 day incubation, fresh medium was added to each well.

To validate the utilization of this platform for 3D tissue culture and the *lux* system as a potential imaging technique, Zeocin, an antibiotic in the bleomycin family, was added in triplicate to the cell-seeded gels following the initial 5 days of 3D structure development to create the

following treatment concentrations: 1800 µg/ml, 1500 µg/ml, 1200 µg/ml, 900 µg/ml, 600 µg/ml, and 300 µg/ml. Additionally, one cell-seeded gel triplicate remained unexposed to serve as a positive control and to provide a subject for long-term monitoring and assessment of the 3D structure's continued dynamics. Bioluminescence was then monitored sing the IVIS Lumina imaging system (Perkin Elmer) with a 10 minute integration time at various intervals over a 96 hour time course while maintaining the plate under standard incubation conditions between readings. Imaging for the positive control was performed similarly, but was continued over 263 hours, concluding when it was no longer statistically differentiable from the negative control. Medium in this well was refreshed after the initial 96 hour screening and every third day afterwards.

Although the Ultra-Low binding plate advertises insignificant cellular attachment, control runs were employed to determine any effects that cells not attached to the hydrogel and not removed by refreshing might have had on the results. Actively growing 2nd generation autobioluminescent HEK293 cells were plated in triplicate on an Ultra-Low binding 96-well plate at the following concentrations: 5.0×10^4 cells/ml, 1.0×10^5 cells/ml, 1.5×10^5 cells/ml, 2.0×10^5 cells/ml, and 2.5×10^5 cells/ml. Subsequently, the plate was incubated for 24 hours at 37 °C and then refreshed to remove any unattached cells, mimicking the hydrogel protocol. However, in this case the spent medium was collected and imaged using a 10 minute integration, and the resultant bioluminescent signal was correlated with the originally plated concentration. After an additional 5 days of incubation, the medium was again refreshed and the plate was imaged to ascertain the bioluminescence of any remaining cells.

Magnetic Levitation Bioassember (N3D Bio)

Actively growing 2nd generation autobioluminescent HEK293 cells growing in 25 cm^2 tissue culture were incubated with 200 µl of the magnetic nanoparticle solution overnight. The cells were then harvested, counted using the Scepter, and resuspended in fresh medium. Approximately 1.0×10^4, 2.5×10^4, 5.0×10^4, 7.5×10^4, 1.0×10^5, 2.5×10^5, and 5.0×10^5 cells in 400 µl volume were plated in duplicate in an Ultra-Low binding 24-well plate (Corning) along with triplicate 400 µl medium only controls. After plating, the magnetic drive and opaque spacer were positioned following manufacturer's protocol. The plate was then incubated at 37 °C with 5% CO_2.

Each well was refreshed every third day by removing old medium and adding 400 µl of fresh medium. To facilitate the integrity of the 3D structure and ensure that cells were not removed during refreshing, the magnetic drive was placed upside-down underneath the plate, magnetically adhering the cells to the bottom of the well. Before repositioning the magnetic drive and opaque spacer above the wells, each was sterilized with 70% ethanol.

Furthermore, the plate was imaged over a 45 day period at various intervals using the IVIS Lumina imaging system. Imaging procedure included removing the magnetic drive and opaque spacer, which did not permit bioluminescence visualization, and a 10 minute integration.

UV Cross-linked Poly-ethylene Glycol Hydrogel

Polymerized polyethylene glycol (PEG) hydrogels have been well-researched and are commonly used for *in vivo* studies because of their biocompatibility across a wide range of matrices[15-17]. Recent studies have shown that polymerization by UV cross-linking may permit

encapsulation of cells in 3D structures, maintaining cell viability[18, 19]. To evaluate this 3D tissue culture technique, several experiments were performed to determine 1) the optimal UV wavelength to allow for cross-linking while maintaining cell viability and bioluminescent emission, 2) the bioluminescent dynamics of the PEG-encapsulated cells, and 3) potential toxicity of the PEG hydrogel.

To determine the optimal UV wavelength for maintaining cell viability and bioluminescence, approximately 2.0×10^5 2nd generation autobioluminescent HEK293 cells along with equal volume of medium were plated in triplicate wells of three 24-well plates, which were immediately imaged using a 10 min integration time in the IVIS Lumina imaging system. Following the initial bioluminescent reading, each of the three plates was exposed to 245 nM or 365 nm UV for 10 minutes, or left unexposed, respectively. The plates were then reimaged using a 10 minute integration to evaluate the effects of UV exposure. This procedure was repeated to include 20 minutes of UV exposure.

To encapsulate the cells, actively growing 2nd generation autobioluminescent HEK293 cells were harvested from 75 cm^2 tissue culture flasks, washed with PBS, counted using the Scepter, and resuspended in the gel precursor solution at a final concentration of 1.0×10^6 or 10^7 cells/ml. The gel precursor solution consisted of 30%, 25%, 20%, or 15% (w/w) PEG and the photoinitiator (4-(2-Hydroxyethoxy) phenyl-(2-hydroxy-2-propyl) ketone) at a final concentration of 30 mg/ml in DMEM medium. Ten microliter of each cell/precursor suspension was then pipetted in duplicate between two sterile glass plates separated by a thin plastic strip, followed by a 10 minute exposure to 365 nm UV to initiate hydrogel formation. The gels that properly developed were transferred to individual wells of in a black 96-well plate and immersed in 200 µl of medium. Equal volumes of medium and unexposed cells were included as negative and positive controls, respectively. Bioluminescence was visualized in the IVIS Lumina imaging system using a 10 minute integration at 30 minute intervals for 21 hours.

Finally, toxicities of the PEG and the photoinitiator were assessed by suspend ~ 1.0×10^4 2nd generation autobioluminescent HEK293 cells in triplicate in 100 µl of the following solutions: DMEM medium, DMEM + 30% PEG, DMEM + 30 mg photoinitiator/ml, and DMEM + 30% PEG + 30 photoinitiaator mg/ml. Bioluminescence was then visualized using a 10 minute integration in the IVIS Lumina imaging system. After imaging, each triplicate was combined and centrifuged at 1250 rpm for 7 minutes. Each pellet was washed with PBS and resuspended in 200 µl of fresh medium and imaged using the same procedure as described above.

Results

Porous Polycaprolactone 3D Scaffold

The bioluminescent activity of the 1st generation autobioluminescent HEK293 cells grown on the Kiyatec polycaprolactone 3D culture scaffolds proved significantly greater than the medium control (student's *t*-test $p < 0.0002$) and those grown as a monolayer ($p < 0.004$) or in suspension ($p < 0.02$). Furthermore, an increasing trend was observed until approximately 8.5 hours at which a steady decrease began (Figure 2). Nevertheless, a drop in bioluminescence that opposes this trend was observed for each sample centered at ~13 hours.

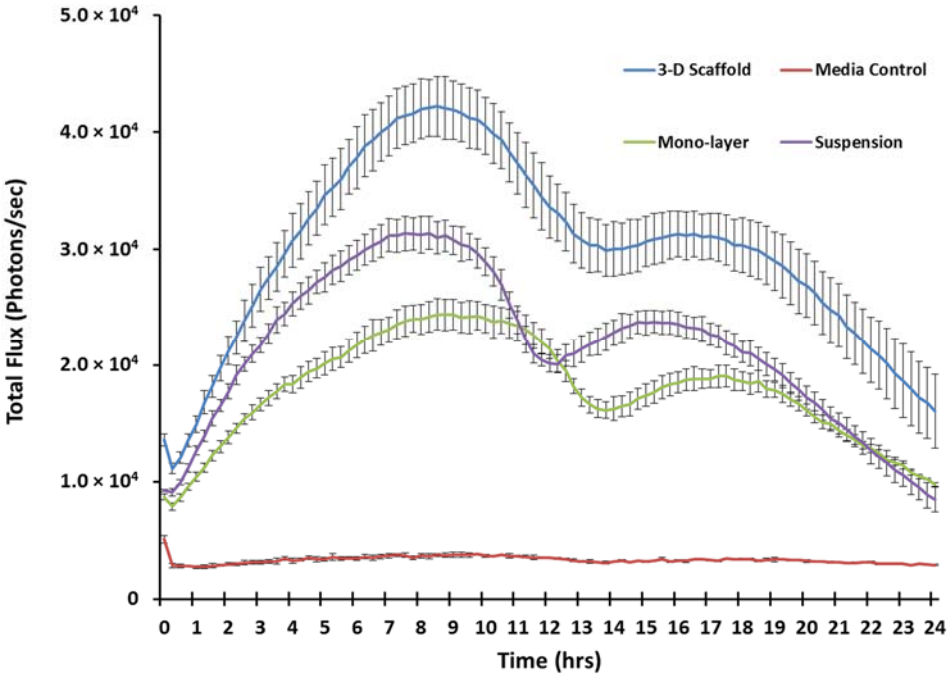

Figure 2. HEK293 cells plated onto the Kiyatec polycaprolactone 3D culture scaffold, in suspension, and in a monolayer. These treatments were imaged over a 24 hour period.

Hyaluronic Acid Gel

Exposure of bioluminescent cells grown on the hyaluronic acid hydrogels to various concentrations of the antibiotic Zeocin ranging from 300 to 1800 µg/ml demonstrated a consistent decreasing trend, eventually becoming non-differentiable from the medium control (Figure 3). However, only a slight correlation was observable between antibiotic concentration and bioluminescence (R^2=0.49 after 24 hours). Nevertheless, bioluminescent signal produced from the unexposed cells remained distinguishable from the medium control throughout the experiment.

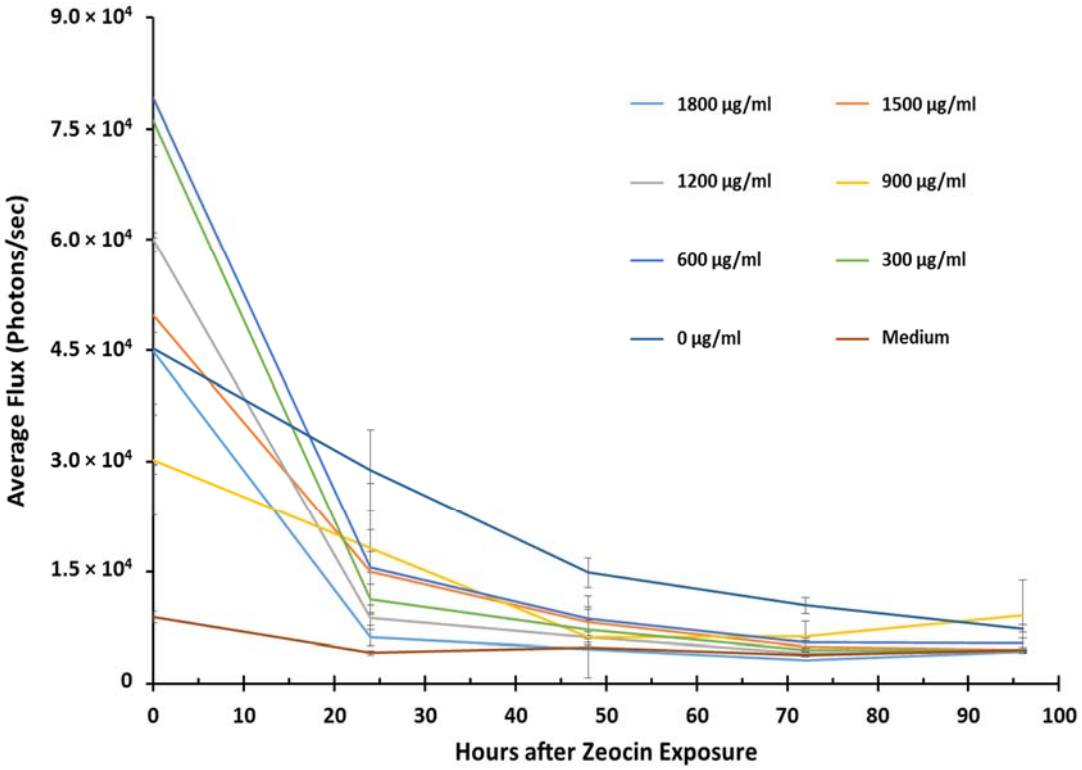

Figure 3. Bioluminescence of 2nd generation autobioluminescent HEK293 cells plated onto Celenys hyaluronic gels and exposed to various concentrations of Zeocin.

Therefore, imaging of the unexposed cells was continued for additional 167 hours to further demonstrate the extended imaging and culturing capabilities of the autobioluminescent cells on the hyaluronic acid hydrogel (Figure 4). Although bioluminescence peaked hours after the 5 day incubation, cell viability and activity were maintained throughout the imaging duration. It must also be noted that an extreme outlier exhibiting bioluminescent activity more than 2.5 times of the maximum demonstrated at the 24 hour time-point was excluded from the 192 hour replicates. To assess any confounding effects from cells attached to plate instead of to the hydrogel, varying numbers of 2nd generation autobioluminescent HEK293 cells were plated in individual wells of an Ultra-Low binding 96-well plate and incubated following manufacturer's protocol. Imaging of the spent medium removed after the suggested one day incubation for cell attachment to the hydrogel revealed bioluminescent signals that correlated well (R^2=0.96) with the number of cells initially plated (Figure 5), suggesting that cell attachment to the plate itself was negligible. Any potentially remaining cells attached to the plate were incubated for 5 days and the resultant bioluminescence

was compared to a medium control. None of the samples demonstrated a significantly differentiable signal (p = 0.288, 0.090, 0.352, 0.059, and 0.061).

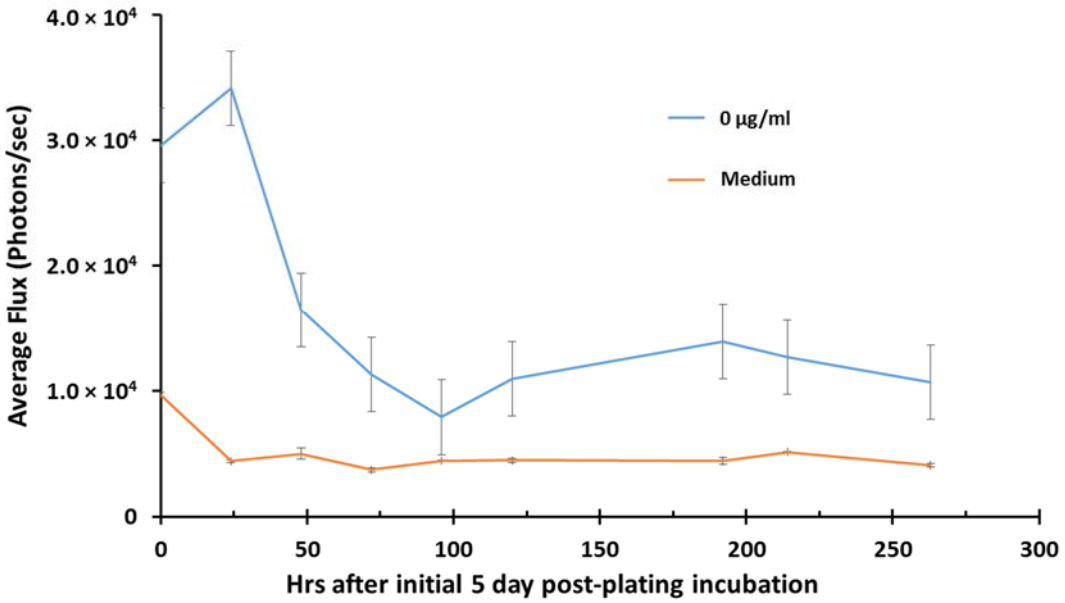

Figure 4. Cells grown on the hyaluronic hydrogel *without Zeocin treatment were imaged* for 263 hours after the 5 day post-plating incubation and demonstrated a signal statistically differentiable from the control throughout.

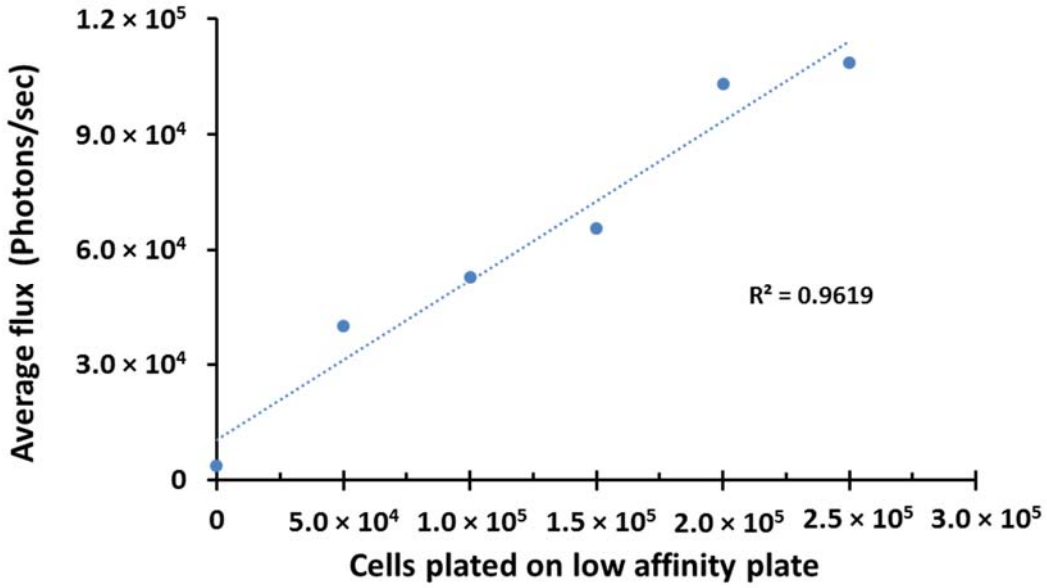

Figure 5. Bioluminescence produced from the spent medium containing unattached cells collected 1 day post plating to an Ultra-Low binding 96-well plate correlated well (R^2=0.96) with the number of cells initially plated.

Magnetic Levitation Bioassember

Cells grown in 3D structures using the N3D magnetic levitation drive were imaged for 45 days (Figure 6). Although the bioluminescence measured throughout the experiment did not demonstrate an observable pattern with respect to concentration plated, the initial bioluminescence at 24 hours after plating correlated well with concentration up to 1.0×10^5 cells (R^2=0.94). The bioluminescent signal of the 5.0×10^5 and 2.5×10^5 sample became statistically non-differentiable from the medium control after 2 and 8 days, respectively. The remaining samples produced a detectable signal throughout the 45 days of experiment.

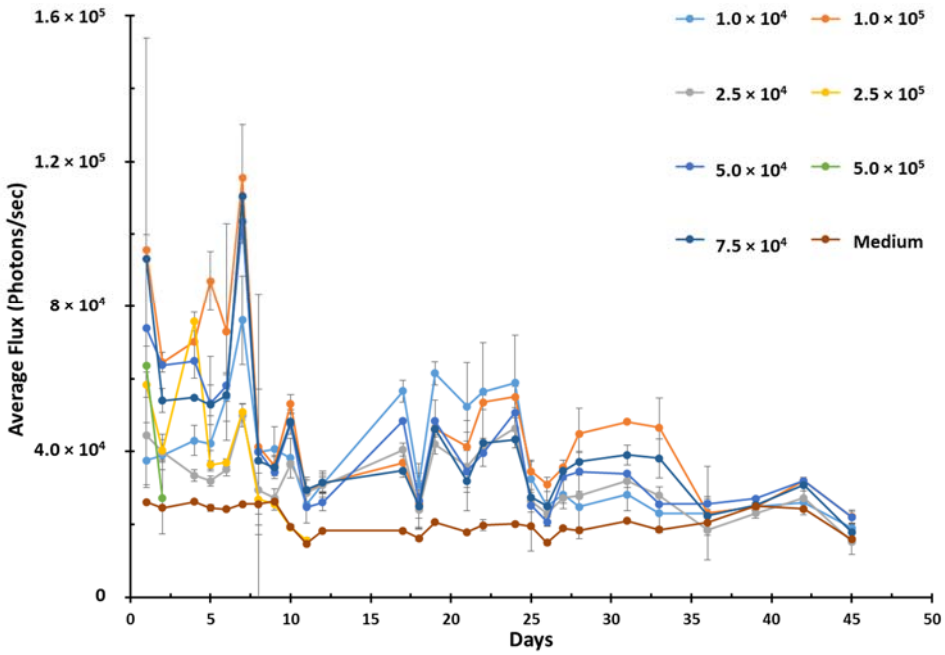

Figure 6. HEK293 cells incubated with magnetic nanoparticles, plated on an Ultra-Low binding plate, and magnetically levitated.

UV Cross-linked PEG Hydrogel

The comparative effects of 254 nm and 365 nm UV on cell viability and bioluminescence were assessed by plating equal number of 2nd generation autobioluminescent HEK293 cells and exposing the samples to different UV treatments (Figure 7). Cells exposed to 20 minutes of 365 nm UV were not statistically differentiable from the unexposed cells ($p = 0.93$). However, after 10 and 20 minutes, cells exposed to 254 nm UV produced significantly smaller bioluminescent signals than the positive control with a more pronounced difference after 20 minutes ($p < 0.001$ and $p < 0.00001$ respectively).

The encapsulation process was then repeated using 365 nm UV and varying concentrations of PEG (Figure 8). Although the positive control consisting of 1.0×10^5 cells in equal volume of DMEM medium demonstrated detectable bioluminescent signals, none of the hydrogel samples was distinguishable from the medium only control regardless of PEG concentration.

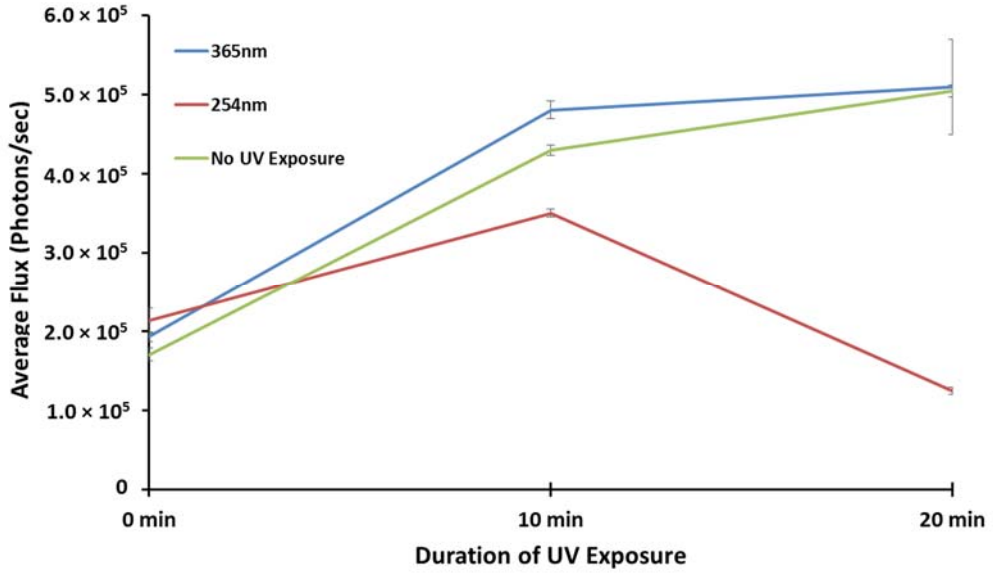

Figure 7. Equal numbers of 2nd generation autobioluminescent HEK293 cells were exposed to different wavelength of UV for two 10 minute increments. A control that was not exposed to any UV was also included.

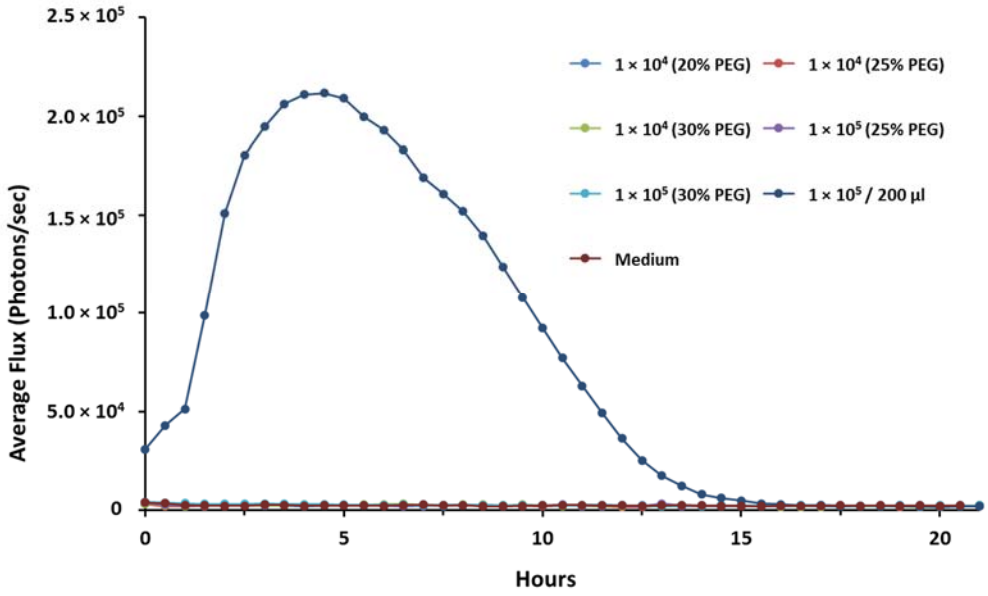

Figure 8. HEK293 cells encapsulated in PEG hydrogels of various concentrations using 365 nm UV. Along with a medium control, a positive control of 1.0×10^5 cells in 200 µl DMEM medium was also included.

Finally, approximately 1.0×10^4 2nd generation autobioluminescent HEK29cells were plated in solutions containing hydrogel reagents at the concentrations used for gel formation (Figure 9). The sample containing cells in medium only produced a statistically significant bioluminescent signal from the medium control ($p = 0.0002$). In contrast, none of the samples containing hydrogel precursor reagents were differentiable from the medium control (photoinitiator: $p = 0.76$, PEG: $p = 0.10$, and photoinitiator + PEG: $p = 0.05$).

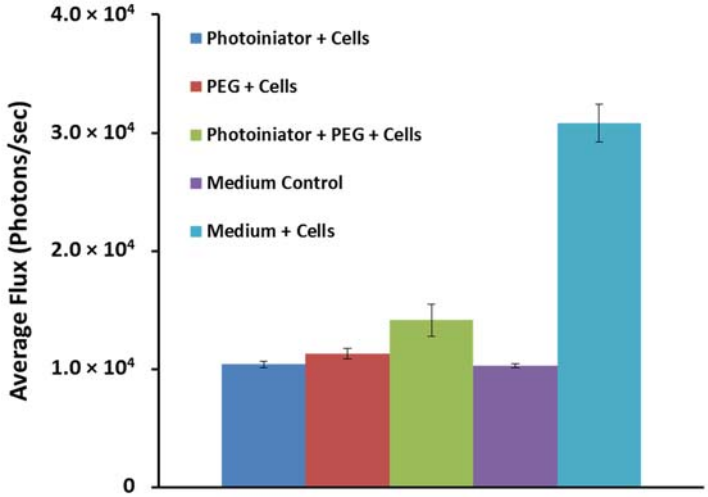

Figure 9. Comparison of bioluminescence produced from equal number (1.0×10^4 of 2nd generation HEK293 cells suspended in various PEG hydrogel precursor solutions without UV exposure.

To evaluate whether the results presented in Figure 9 stemmed from cytotoxicity or UV absorbance, the samples were collected, washed with PBS, and resuspended in fresh medium. No bioluminescent signal was observable for any treatment except for cells that were not exposed to hydrogel precursor reagents (Figure 10).

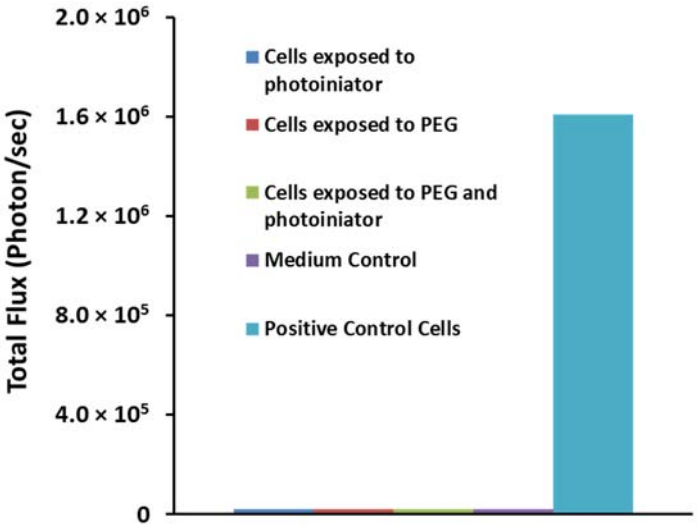

Figure 10. The cells from Figure 9 were washed, replated, and imaged. Only the cells that were previously plated in simple medium demonstrated a detectable bioluminescent signal.

Discussion

Utilizing an autonomously bioluminescent HEK293 cell line, the polycaprolactone 3D tissue scaffold was compared to traditional monolayer and suspension cultures. Since the health and metabolic activity of the cells had previously been correlated with bioluminescent signal and the purpose of pursuing 3D tissue culture is to provide an environment that mimics *in vivo* conditions, the resultant signal dynamics represent the cellular differences created by these dissimilar culture techniques[20]. Signifying dynamics that were previously unmeasurable due to technological and imaging limitations, this data demonstrates the feasibility of using the *lux* cassette as a 3D culture imaging tool. Furthermore, the activity and growth of cells demonstrated by these results validate the potential of this scaffold as a 3D culture platform. The metabolic activity as measured through bioluminescent signal for cells plated on the 3D scaffold was statistically higher than the suspension and monolayer cultures, highlighting the differences between traditional culture techniques and *in vivo* conditions. As numerous studies have shown, these differences can be pronounced and are the principal reason for culture technique comparison [21, 22].

The bioluminescent activity of the cells plated on hyaluronic acid hydrogels and exposed to the antibiotic Zeocin only demonstrated a minor measurable pattern. Although bioluminescent activity was detectable and all samples tended towards the medium control, antibiotic concentration was not correlated well with any particular change in bioluminescence, divergent from similar studies utilizing the same conditions in 2D culture[23]. Cytotoxicity and drug screening studies have shown that 3D culture more closely resembles *in vivo* clinical studies in drug efficacy, resulting from networked intercellular interactions and a greater resistance to toxic compounds[24, 25]. Thus, the unpatterned results of Zeocin on the hyaluronic acid hydrogel-based 3D cultures may plausibly be explained by the heterogeneity of the 3D culture and increased resistance to damaging environmental conditions and the stability of *in vivo*-like systems.

However, the positive control that was not exposed to any antibiotic continued producing a detectable bioluminescent signal as expected. Further imaging revealed a statistically significant signal throughout and an increase in bioluminescent activity after the wells' first medium refresh. Demonstrating the hyaluronic acid hydrogel's capability for extended culture and the potentially related cyclical dynamics of nutrient use and replacement, the *lux*-based autobioluminescent cells were further validated as a capable tool for 3D culture evaluation.

To identify any potential confounding effects caused by cells that unexpectedly attached to the Ultra-Low binding plate, a range of concentrations were plated and incubated following the Celenys protocol. The spent medium removed after the 1 day incubation required for attachment to the hyaluronic hydrogel produced detectable bioluminescent signals at all concentrations. Furthermore, these signals correlated well with the concentrations originally plated, suggesting that the cells plated were predominantly recovered. However, to fully discount unintentional attachment, the entire Celenys protocol was completed and the plate imaged. Since no detectable signal was observed for any of the concentrations, the hyaluronic hydrogel results appeared to be unaffected by inadvertent attachment. As previous studies have shown, these unidentified attachments can interfere significantly with accurate signal detection[26]. The cells used in this experiment have demonstrated detectable signals at quantities as low as 10^3, suggesting that even a small fraction of plated cells adhering to an attachment resistant plate could bias results.

In opposition to providing cells with a physical scaffold, levitation using magnetic nanoparticles bound to target cells has been proposed to create 3D structures that mimic natural conditions[27]. In this experiment, most of the cells cultured and plated using the magnetic bioassembler demonstrated detectable bioluminescent signal over a 45 day period. However, the 5.0×10^5 and 2.5×10^5 samples respectively stopped producing a detectable signal after 2 and 8 days, indicating a maximum capacity for maintaining proper cellular health. Furthermore, although research suggests that cells will detach and grow independent from the magnetic nanoparticles after 8 days, careful handling promoted the maintenance of the 3D structure for approximately 45 days. Further research and experimentation will be required to accurately elucidate applicable conclusions since only minor patterns were observed from this data, but the signal dynamics demonstrated substantiate the long-term imaging and culturing capabilities of the autobioluminescent cells and magnetic levitation systems.

In addition to the 3D culture techniques discussed above, UV cross-linkable PEG hydrogel was also evaluated in this study. Although both 254 nm and 365 nm UV exposure are effective in PEG hydrogel formation, cells exposed to 245 nm UV displayed a significant decrease in bioluminescent signal relative to those exposed to 365 nm UV. Given that 254 nm UV is a known and prevalently used microbicidal instrument, the absence of bioluminescent activity was plausibly attributed to UV damage[28]. Since exposure 365 nm UV had minimal effect on bioluminescent emission (Figure 7), the encapsulation process was evaluated using 365 nm low energy UV exposure. Additionally, the PEG concentration was varied with hopes of improving cell viability during the encapsulation process. Although the literature used as a blueprint for encapsulation states that 30% (w/w) PEG maintains cellular health, other studies have shown that PEG concentrations above 10% can be damaging[18, 19, 29]. Increasing PEG concentrations result in a firmer and more easily manipulated gel but the dense polymer limits nutrient diffusion for long term viability and increases free-radical concentrations during gel formation. However, after 21 hours of continuous imaging, no detectable bioluminescent signal was observed for any of the PEG concentrations, whereas, the positive controls of 10^5 cells resuspended in 10 µl medium demonstrated significant bioluminescent activity.

The cells were then suspended in solutions containing one or both of the hydrogel reagents at the same concentrations used for gel formation without UV exposure to evaluate potential negative impacts on bioluminescent activity. The samples containing these reagents were not differentiable from the medium control whereas cells plated in medium were statistically greater. Furthermore, subsequent washing of these cells and replating in medium did not affect bioluminescent activity, suggesting that the compounds are toxic and not simply absorbing the bioluminescent signal, a plausible hypothesis given the photo-active nature of the polymerization initiating reagent.

In conclusion, the UV cross-linked PEG hydrogel did not prove successful. Encapsulation of autobioluminescent cells using high and low energy UV exposure and various PEG concentrations did not demonstrate a detectable bioluminescent signal. Thus, subsequent research may endeavor to evaluate additional encapsulation methods. Although free radical cross-linking remains a significant challenge to cell viability, various chemically cross-linked gels have demonstrated potential encapsulation application without the use of free-radical polymerization. For example, gel formation using collagen backbones and chemically induced cross-linking has been demonstrated and is commercially available[30]. Preliminary research conducted using this encapsulation process appears promising. Although inconsistent, encapsulation has been achieved

while maintaining cell viability and bioluminescent activity (Figure 11). Current experimentation endeavors to evaluate a commercially available protocol and alter it for consistent encapsulation of autobioluminescent HCT116 cells. The success of these experiments will serve to validate the *lux* cassette's use for imaging 3D encapsulation matrices.

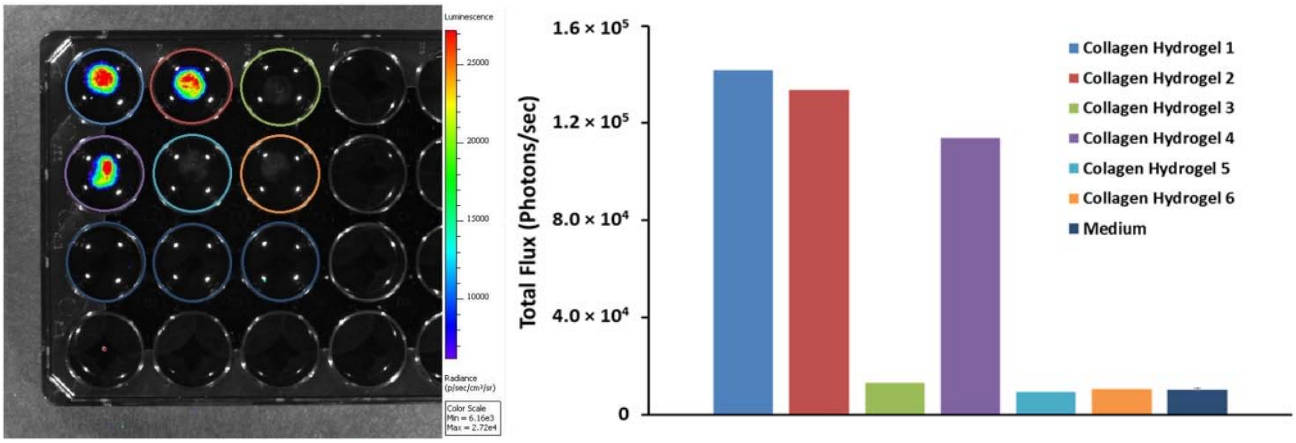

Figure 11. Preliminary collagen encapsulation of the autobioluminescent HCT116 cells.

References

1. Williams, T. M., Burlein, J. E., Ogden, S., Kricka, L. J., and Kant, J. A. (1989) Advantages of Firefly Luciferase as a Reporter Gene - Application to the Interleukin-2 Gene Promoter, *Anal Biochem 176*, 28-32.
2. Baschong, W., Suetterlin, R., and Laeng, R. H. (2001) Control of autofluorescence of archival formaldehyde-fixed, paraffin-embedded tissue in confocal laser scanning microscopy (CLSM), *J Histochem Cytochem 49*, 1565-1571.
3. Chaorattanakawee, S., Tyner, S. D., Lon, C., Yingyuen, K., Ruttvisutinunt, W., Sundrakes, S., Saignam, P., Johnson, J. D., Walsh, D. S., Saunders, D. L., and Lanteri, C. A. (2013) Direct comparison of the histidine-rich protein-2 enzyme-linked immunosorbent assay (HRP-2 ELISA) and malaria SYBR green I fluorescence (MSF) drug sensitivity tests in Plasmodium falciparum reference clones and fresh ex vivo field isolates from Cambodia, *Malaria journal 12*, 239.
4. Zhang, C., Yan, Z., Arango, M. E., Painter, C. L., and Anderes, K. (2009) Advancing bioluminescence imaging technology for the evaluation of anticancer agents in the MDA-MB-435-HAL-Luc mammary fat pad and subrenal capsule tumor models, *Clinical cancer research : an official journal of the American Association for Cancer Research 15*, 238-246.
5. Close, D. M., Patterson, S. S., Ripp, S., Baek, S. J., Sanseverino, J., and Sayler, G. S. (2010) Autonomous Bioluminescent Expression of the Bacterial Luciferase Gene Cassette (lux) in a Mammalian Cell Line, *PloS one 5*.
6. Baggett, B., Roy, R., Momen, S., Morgan, S., Tisi, L., Morse, D., and Gillies, R. J. (2004) Thermostability of Firefly Luciferases Affects Efficiency of Detection by In Vivo Bioluminescence, *Mol Imaging 3*, 324-332.
7. Dewet, J. R., Wood, K. V., Deluca, M., Helinski, D. R., and Subramani, S. (1987) Firefly Luciferase Gene - Structure and Expression in Mammalian-Cells, *Mol Cell Biol 7*, 725-737.
8. Close, D. M., Xu, T., Sayler, G. S., and Ripp, S. (2011) In vivo bioluminescent imaging (BLI): noninvasive visualization and interrogation of biological processes in living animals, *Sensors 11*, 180-206.
9. Xu, T. (2012) Optimization of Bacterial Bioluminescence (*lux*) Expression and Development of Autonomous *lux*-Based Reporters in Human Cell Lines, In *Microbiology*, The Univeristy of Tennessee.
10. Mudge, S., LewisHenderson, W., and Birch, R. (1996) Comparison of Vibrio and firefly luciferases as reporter gene systems for use in bacteria and plants, *Australian Journal of Plant Physiology 23*, 75-83.
11. Bhadriraju, K., and Chen, C. S. (2002) Engineering cellular microenvironments to improve cell-based drug testing, *Drug discovery today 7*, 612-620.
12. Bissell, M. J., Radisky, D. C., Rizki, A., Weaver, V. M., and Petersen, O. W. (2002) The organizing principle: microenvironmental influences in the normal and malignant breast, *Differentiation; research in biological diversity 70*, 537-546.
13. Simon, K. A., Park, K. M., Mosadegh, B., Subramaniam, A. B., Mazzeo, A. D., Ngo, P. M., and Whitesides, G. M. (2014) Polymer-based mesh as supports for multi-layered 3D cell culture and assays, *Biomaterials 35*, 259-268.
14. Pampaloni, F., Reynaud, E. G., and Stelzer, E. H. K. (2007) The third dimension bridges the gap between cell culture and live tissue, *Nat Rev Mol Cell Bio 8*, 839-845.
15. Ozcelik, B., Brown, K. D., Blencowe, A., Daniell, M., Stevens, G. W., and Qiao, G. G. (2013) Ultrathin chitosan-poly(ethylene glycol) hydrogel films for corneal tissue engineering, *Acta biomaterialia 9*, 6594-6605.
16. Gupta, A., Upadhyay, N. K., Parthasarathy, S., Rajagopal, C., and Roy, P. K. (2013) Nitrofurazone-loaded PVA-PEG semi-IPN for application as hydrogel dressing for normal and burn wounds, *Journal of Applied Polymer Science 128*, 4031-4039.

17. Zhu, J. M. (2010) Bioactive modification of poly(ethylene glycol) hydrogels for tissue engineering, *Biomaterials 31*, 4639-4656.
18. Cai, L., Lu, J., Sheen, V., and Wang, S. F. (2012) Optimal Poly(L-lysine) Grafting Density in Hydrogels for Promoting Neural Progenitor Cell Functions, *Biomacromolecules 13*, 1663-1674.
19. Cai, L., Lu, J., Sheen, V., and Wang, S. F. (2012) Promoting Nerve Cell Functions on Hydrogels Grafted with Poly(L-lysine), *Biomacromolecules 13*, 342-349.
20. Close, D. M., Webb, J., Ripp, S., Patterson, S. S., and Sayler, G. S. (2012) Remote Detection of Human Toxicants in Real Time using a Human Optimized Bioluminescent Bacterial Luciferase Gene Cassette Bioreporter, *Sensing Technologies for Global Health, Militairy Medicine, Disaster Response, and Environmental Monitoring II 8371*.
21. Haycock, J. W. (2011) 3D cell culture: a review of current approaches and techniques, *Methods in molecular biology 695*, 1-15.
22. Prestwich, G. D. (2007) Simplifying the extracellular matrix for 3-D cell culture and tissue engineering: a pragmatic approach, *Journal of cellular biochemistry 101*, 1370-1383.
23. Xu, T., Close, D. M., Webb, J., Ripp, S., and Sayler, G. S. (2013) Autonomously Bioluminescent Mammalian Cells for Continous and Real-time Monitoring of Cytotoxicity, *Journal of Visualized Experiments*.
24. Fey, S. J., and Wrzesinski, K. (2012) Determination of drug toxicity using 3D spheroids constructed from an immortal human hepatocyte cell line, *Toxicological sciences : an official journal of the Society of Toxicology 127*, 403-411.
25. Yip, D., and Cho, C. H. (2013) A multicellular 3D heterospheroid model of liver tumor and stromal cells in collagen gel for anti-cancer drug testing, *Biochemical and biophysical research communications 433*, 327-332.
26. Brault, N. D., Gao, C., Xue, H., Piliarik, M., Homola, J., Jiang, S., and Yu, Q. (2010) Ultra-low fouling and functionalizable zwitterionic coatings grafted onto SiO2 via a biomimetic adhesive group for sensing and detection in complex media, *Biosensors & bioelectronics 25*, 2276-2282.
27. Haisler, W. L., Timm, D. M., Gage, J. A., Tseng, H., Killian, T. C., and Souza, G. R. (2013) Three-dimensional cell culturing by magnetic levitation, *Nature protocols 8*, 1940-1949.
28. Coohill, T. P., and Sagripanti, J. L. (2008) Overview of the inactivation by 254 nm ultraviolet radiation of bacteria with particular relevance to biodefense, *Photochemistry and photobiology 84*, 1084-1090.
29. Burdick, J. A., and Anseth, K. S. (2002) Photoencapsulation of osteoblasts in injectable RGD-modified PEG hydrogels for bone tissue engineering, *Biomaterials 23*, 4315-4323.
30. Sadeghi, M., and Hosseinzadeh, H. (2013) SYNTHESIS AND PROPERTIES OF COLLAGEN-g-POLY(SODIUM ACRYLATE-co-2-HYDROXYETHYLACRYLATE) SUPERABSORBENT HYDROGELS, *Braz J Chem Eng 30*, 379-389.